Antiproton scattering off ^{3}He and ^{4}He nuclei at low and intermediate energies

Yu. N. Uzikov,[1] J. Haidenbauer,[2,3] and B. A. Prmantayeva[4]
[1]*Laboratory of Nuclear Problems, Joint Institute for Nuclear Research, 141980 Dubna, Russia*
[2]*Institute for Advanced Simulation, Forschungszentrum Jülich, D-52425 Jülich, Germany*
[3]*Institut für Kernphysik and Jülich Center for Hadron Physics, Forschungszentrum Jülich, D-52425 Jülich, Germany*
[4]*L.N. Gumilyov Eurasian National University, 010008 Astana, Kazakhstan*
(Received 21 July 2011; published 28 November 2011)

Antiproton scattering off ^{3}He and ^{4}He targets is considered at beam energies below 300 MeV within the Glauber-Sitenko approach, utilizing the $\bar{N}N$ amplitudes of the Jülich model as input. A good agreement with available data on differential $\bar{p}\,^4$He cross sections and on $\bar{p}\,^3$He and $\bar{p}\,^4$He reaction cross sections is obtained. Predictions for polarized total $\bar{p}\,^3$He cross sections are presented, calculated within the single-scattering approximation and including Coulomb-nuclear interference effects. The kinetics of the polarization buildup is discussed.

DOI: 10.1103/PhysRevC.84.054011 PACS number(s): 13.75.Cs, 24.70.+s, 25.43.+t, 29.27.Hj

I. INTRODUCTION

One of the projects suggested for the future FAIR facility in Darmstadt comes from the PAX collaboration [1]. Its aim is to measure the proton transversity in the interaction of polarized antiprotons with protons. In order to produce an intense beam of polarized antiprotons, the collaboration intends to use antiproton elastic scattering off a polarized hydrogen target (^{1}H) in a storage ring [2]. The basic idea is connected to the result of the FILTEX experiment [3], where a sizable effect of polarization buildup was achieved in a storage ring by scattering of unpolarized protons off polarized hydrogen atoms at low beam energies of 23 MeV. Recent theoretical analyses [4–7] have shown that the polarization buildup observed in Ref. [3] can be understood quantitatively. According to those authors it is solely due to the spin dependence of the hadronic (proton-proton) interaction which leads to the so-called spin-filtering mechanism, i.e., to a different rate of removal of beam protons from the ring for different polarization states of the target proton.

The antinucleon-nucleon ($\bar{N}N$) interaction has been studied quite extensively over the past 3 decades or so [8–14], not least because of the wealth of data collected at the Low Energy Antiproton Ring (LEAR) facility at CERN (cf. the reviews [15–17]). Still, one has to concede that, in contrast to the NN case, up to now the spin dependence of the $\bar{N}N$ interaction is fairly poorly known. Therefore, it is an open question whether any sizable polarization buildup can also be achieved in case of an antiproton beam based on the spin-filtering mechanism. Indeed, recently several theoretical studies were performed with the aim to estimate the expected polarization buildup for antiprotons, employing different $\bar{p}p$ interactions [18–20]. In addition to using polarized protons as target one could also use light nuclei as possible source for the antiproton polarization buildup. Corresponding investigations for antiproton scattering on a polarized deuteron target were presented in Refs. [19,21,22]. As was shown in Refs. [19,21] on the basis of the Glauber-Sitenko theory [23,24] with elementary $\bar{p}N$ amplitudes taken from the Jülich $\bar{N}N$ models [11,13,25,26], the $\bar{p}d$ interaction could provide a comparable or even more effective way than the $\bar{p}p$ interaction to obtain polarized antiprotons. This conjecture can be checked at a planned experiment [27] at the Antiproton Decelerator (AD) facility at CERN.

Yet another option could be the scattering of antiprotons off a polarized ^{3}He target. Since the polarization of the ^{3}He nucleus is carried mainly by the neutron, the $\bar{p}n$ amplitudes are expected to dominate the spin observables of this reaction. In the present work we calculate spin-dependent cross sections for the $\bar{p}\,^3$He interaction on the basis of an approach similar to that developed in Ref. [19]. Experimental information on $\bar{p}\,^3$He scattering is rather sparse [28,29]. Thus, in order to examine the validity of the employed Glauber-Sitenko approach [24,30] at low and intermediate energies we consider here also the $\bar{p}\,^4$He system where the PS179 collaboration has performed several measurements [31–38] at the LEAR facility at CERN. In particular, we calculate differential cross sections for elastic scattering and compare them with data available at beam momenta of 200 MeV/c [37] and 600 MeV/c [36]. As far as we know, this is the first time that those PS179 data are analyzed within an approach that utilizes elementary $\bar{N}N$ amplitudes taken from a microscopic model of the $\bar{N}N$ interaction. Though a few investigations of $\bar{p}\,^3$He and $\bar{p}\,^4$He scattering have been performed before [39,40] based on the Glauber-Sitenko theory, none of them connects directly with amplitudes generated from potential models that are fitted to $\bar{N}N$ data.

The article is structured as follows: In Sec. II some details of the formalism are given. In particular, we define the amplitudes and their relation to the cross sections and we provide the relation between the amplitudes of the $\bar{p}\,^3$He system with those of the elementary $\bar{N}N$ interaction within the single-scattering approximation. Expressions required for the inclusion of the Coulomb interaction are also provided. In Sec. III predictions for $\bar{p}\,^3$He and $\bar{p}\,^4$He are given, obtained within the Glauber-Sitenko approach. The results are compared with the available data for those systems. In Sec. IV the polarization efficiency for $\bar{p}\,^3$He is studied. We introduce the pertinent quantities and then present and discuss the numerical results. The article closes with a short summary.

II. FORMALISM

A. Forward elastic $\bar{p}\,^3$He scattering amplitude and total cross sections

In order to calculate the total unpolarized and spin-dependent $\bar{p}\,^3$He cross sections we use the optical theorem. If $\hat{F}(\theta = 0)$ is the operator of forward elastic scattering for $\bar{p}\,^3$He and ρ is the spin-density matrix of the $\bar{p}\,^3$He system, then the total cross section, σ, is given by

$$\sigma = \frac{4\pi}{k_{\bar{p}\tau}} \mathrm{Im} \frac{\mathrm{Tr}\rho \hat{F}(0)}{\mathrm{Tr}\rho}, \tag{1}$$

where $k_{\bar{p}\tau}$ is the modulus of the center-of-mass (c.m.) momentum in the $\bar{p}\,^3$He system. The spin-density matrix for the $\bar{p}\,^3$He system is

$$\rho = \frac{1 + \boldsymbol{\sigma}_{\bar{p}} \mathbf{P}_{\bar{p}}}{2} \frac{1 + \boldsymbol{\sigma}_{\tau} \mathbf{P}_{\tau}}{2}, \tag{2}$$

where $\boldsymbol{\sigma}_{\bar{p}}$ and $\boldsymbol{\sigma}_{\tau}$ are Pauli matrices acting on the $\bar{p}$ and ^{3}He spin states, respectively, and $\mathbf{P}_{\bar{p}}$ ($\mathbf{P}_{\tau}$) is the polarization vector of the antiproton (^{3}He). While, in general, elastic scattering of two nonidentical spin-$\frac{1}{2}$ particles involves six complex amplitudes [41], only three of those contribute at forward direction. Thus, the operator $\hat{F}(0)$ can be written in the form [42],

$$\hat{F}(0) = F_0 + F_1 \boldsymbol{\sigma}_{\bar{p}} \cdot \boldsymbol{\sigma}_{\tau} + F_2 (\boldsymbol{\sigma}_{\bar{p}} \cdot \hat{\mathbf{k}})(\boldsymbol{\sigma}_{\tau} \cdot \hat{\mathbf{k}}), \tag{3}$$

where F_0, F_1, F_2 are complex amplitudes and $\hat{\mathbf{k}}$ is the unit vector along the beam direction. Inserting Eqs. (2) and (3) into Eq. (1) one obtains

$$\sigma = \sigma_0 + \sigma_1 \mathbf{P}_{\bar{p}} \cdot \mathbf{P}_{\tau} + \sigma_2 (\mathbf{P}_{\bar{p}} \cdot \hat{\mathbf{k}})(\mathbf{P}_{\tau} \cdot \hat{\mathbf{k}}), \tag{4}$$

where the total unpolarized cross section σ_0 and the total spin-dependent cross sections σ_1 and σ_2 are introduced as

$$\sigma_0 = \frac{4\pi}{k_{\bar{p}\tau}} \mathrm{Im} F_0, \tag{5}$$

$$\sigma_1 = \frac{4\pi}{k_{\bar{p}\tau}} \mathrm{Im} F_1, \tag{6}$$

$$\sigma_2 = \frac{4\pi}{k_{\bar{p}\tau}} \mathrm{Im} F_2. \tag{7}$$

B. Single-scattering approximation

For the ground state of the ^{3}He nucleus we use the completely antisymmteric wave function $\Psi^A(1, 2, 3)$ defined within the isospin formalism. Only the fully symmetric spatial part, Ψ_X^S, and the antisymmetric spin-isospin part, ξ^a, are kept here [43],

$$\Psi^A = \Psi_X^S \xi^a, \tag{8}$$

$$\xi^a = \frac{1}{\sqrt{2}} (\chi' \zeta'' - \chi'' \zeta'), \tag{9}$$

where χ', χ'' are spin functions and ζ', ζ'' are those for the isospin. For the z projection of the ^{3}He spin, $M_S = +\frac{1}{2}$, one has the following spin-wave functions,

$$\chi' = \frac{1}{\sqrt{2}} \alpha(1)[\alpha(2)\beta(3) - \beta(2)\alpha(3)], \tag{10}$$

$$\chi'' = \frac{1}{\sqrt{6}} \alpha(1)[\alpha(2)\beta(3) + \beta(2)\alpha(3)] - \sqrt{\frac{2}{3}} \beta(1)\alpha(2)\alpha(3), \tag{11}$$

where χ' is antisymmetric and χ'' is symmtric with respect to the permutation of the nucleons with the numbers 2 and 3. In Eqs. (10) and (11) the quantity $\alpha(i)$ [$\beta(i)$] corresponds to the eigenvalue of the σ_z operator $+1$ (-1) for the i th nucleon. For the ^{3}He spin projection $M_S = -\frac{1}{2}$ one should interchange $\alpha(1)$ and $\beta(1)$ in Eqs. (10) and (11) and replace $\alpha(2) \to \beta(2)$, $\alpha(3) \to \beta(3)$ in Eq. (11). The isospin-wave functions ζ' and ζ'' are similar to those in Eqs. (10) and (11).

In the single-scattering approximation the operator $\hat{F}$ of $\bar{p}\,^3$He scattering is taken within the isospin formalism as the following sum:

$$\hat{F} = \frac{m_\tau}{m_N} \sqrt{\frac{s_{\bar{p}N}}{s_{\bar{p}\tau}}} [\hat{f}(1) + \hat{f}(2) + \hat{f}(3)], \tag{12}$$

where the $\hat{f}(j)$'s ($j = 1,2,3$) are operators in the $\bar{p}N$ spin-isospin space,

$$\hat{f}(j) = \tfrac{1}{2}(1 + \tau_{z\,j}) \hat{f}^p + \tfrac{1}{2}(1 - \tau_{z\,j}) \hat{f}^n\,. \tag{13}$$

Here m_N (m_τ) is the mass of the nucleon (^{3}He), $\sqrt{s_{\bar{p}N}}$($\sqrt{s_{\bar{p}\tau}}$) the invariant mass of the $\bar{p}N$ ($\bar{p}^3$He) system and $\hat{f}^p$ ($\hat{f}^n$) is the operator related to $\bar{p}p$ ($\bar{p}n$) scattering with the same spin structure as given in Eq. (3), namely

$$\hat{f}^N(0) = f_0^N + f_1^N \boldsymbol{\sigma}_{\bar{p}} \cdot \boldsymbol{\sigma}_N + f_2^N (\boldsymbol{\sigma}_{\bar{p}} \cdot \hat{\mathbf{k}})(\boldsymbol{\sigma}_N \cdot \hat{\mathbf{k}}), \tag{14}$$

where f_i ($i = 0,1,2$) are complex amplitudes. The matrix element of the operator $\hat{F}$ at zero scattering angle is

$$\begin{aligned} &\langle \sigma'_{\bar{p}} M'_S | F_{\bar{p}\,^3\mathrm{He}} | \sigma_{\bar{p}} M_S \rangle \\ &\quad = 3 \frac{m_\tau}{m_N} \sqrt{\frac{s_{\bar{p}N}}{s_{\bar{p}\tau}}} \langle \Psi_x^s | \Psi_x^s \rangle \\ &\qquad \times \left(\frac{1}{6} \langle \chi' | \hat{f}^p | \chi' \rangle + \frac{1}{2} \langle \chi'' | \hat{f}^p | \chi'' \rangle + \frac{1}{3} \langle \chi' | \hat{f}^n | \chi' \rangle \right). \end{aligned} \tag{15}$$

The spin algebra gives, from Eqs. (12), (13), (15) using (8), (9), (10), and (11),

$$F_0 = \frac{k_{\bar{p}\tau}}{k_{\bar{p}N}} \left(2 f_0^p + f_0^n\right), \quad F_1 = -\frac{k_{\bar{p}\tau}}{k_{\bar{p}N}} f_1^n,$$

$$F_2 = \frac{k_{\bar{p}\tau}}{k_{\bar{p}N}} \left(2 f_1^n + f_2^n\right). \tag{16}$$

Here $k_{\bar{p}N}$ is the center-of-mass momentum in the $\bar{p}N$ system which is related to the $\bar{p}\,^3$He momentum $k_{\bar{p}\tau}$ by

$$\frac{m_\tau}{m_N} \sqrt{\frac{s_{\bar{p}N}}{s_{\bar{p}\tau}}} = \frac{k_{\bar{p}\tau}}{k_{\bar{p}N}}, \tag{17}$$

which is valid for equal ($\bar{p}$) beam momenta in the $\bar{p}N$- and $\bar{p}\,^3$He systems. One can see from Eq. (16) that within the single-scattering approximation the spin-dependent cross

sections σ_1 and σ_2 are determined only by $\bar{p}$ scattering off the neutron. This result is in agreement with the fact that the matrix element of the operator of the z projection of the ^{3}He spin, S_z, written as

$$S_z = \sum_{j=1}^{j=3} \left\{ s_z^p(j)\frac{1}{2}[1+\tau_z(j)] + s_z^n(j)\frac{1}{2}[1-\tau_z(j)] \right\} \quad (18)$$

and sandwiched between the ground-state wave function (8) of ^{3}He, is completely determined by the contribution of the z projection of the spin operator of the neutron, s_z^n, whereas the proton operator s_z^p gives zero contribution: $\langle \Psi^A_{M_S} | S_z | \Psi^A_{M_S} \rangle = M_S$, where $M_S = \pm\frac{1}{2}$.

When substituting Eqs. (16) into Eqs. (5), (6), and (7), one can find for the total $\bar{p}\,^3$He cross sections in single-scattering approximation (impulse approximation)

$$\sigma_0^{IA} = \left(2\sigma_0^{\bar{p}p} + \sigma_0^{\bar{p}n}\right)\widetilde{w}, \quad (19)$$

$$\sigma_1^{IA} = -\sigma_1^{\bar{p}n}\,\widetilde{w}, \quad (20)$$

$$\sigma_2^{IA} = \left(2\sigma_1^{\bar{p}n} + \sigma_2^{\bar{p}n}\right)\widetilde{w}, \quad (21)$$

where $\widetilde{w} = \langle \Psi_x^s | \Psi_x^s \rangle$. In the actual calculation we set $\langle \Psi_x^s | \Psi_x^s \rangle = 1$. The total $\bar{p}N$ cross sections $\sigma_i^{\bar{p}N}$ $(i = 0, 1, 2)$ are determined in Ref. [42] in the same way as in Eq. (4) and their relations with the zero-angle elastic-scattering amplitudes f_0, f_1, f_2 can be found in Ref. [42]. Note that in Ref. [4] a different definition for the total polarized cross sections σ_i $(i = 1,2)$ is used where then those quantities actually correspond directly to the transversal and longitudinal cross sections. Their cross sections $(\sigma_{i\,(MS)})$ are related to ours via $\sigma_1 = \sigma_{1\,(MS)}$, $\sigma_2 = \sigma_{2\,(MS)} - \sigma_{1\,(MS)}$. Eqs. (19) and (20) are not changed when being rewritten in terms of $\sigma_{i\,(MS)}$, but Eq. (21) takes then the form $\sigma_{2\,(MS)}^{IA} = \sigma_{2\,(MS)}^{\bar{p}n}$.

C. Coulomb effects

Coulomb effects are sizable at low energies, i.e., for $T_{\rm lab} \leqslant 25$ MeV, as can be seen from the analysis of the FILTEX experiment [2] in which protons were scattered off polarized hydrogen at 23 MeV. For $\bar{p}\,^3$He scattering, Coulomb effects could be even more important due to the twice-as-large electric charge of ^{3}He.

The Coulomb amplitude of elastic $\bar{p}\,^3$He scattering is [44]

$$f_c(\theta) = -\left[\frac{\eta}{2k_{\bar{p}\tau}\sin^2(\theta/2)}\right]\exp\left[i\eta\ln\sin^{-2}(\theta/2) + 2i\tilde{\sigma}_0\right]. \quad (22)$$

Here $\eta = Z_1 Z_2 \alpha \mu_{\bar{p}\tau}/k_{\bar{p}\tau}$, with $Z_1 Z_2 = -2$, α is the fine structure constant and $\mu_{\bar{p}\tau}$ is the reduced mass of the $\bar{p}\,^3$He system. The Coulomb phase is given by $\tilde{\sigma}_0 = \arg\Gamma(1+i\eta)$, where $\Gamma(z)$ is the gamma function.

The total unpolarized Coulomb cross section σ_0^C is estimated here following Ref. [4], where proton-proton scattering in storage rings was analyzed. It leads to the following result:

$$\sigma_0^C = \pi\left(\frac{4\alpha\mu_{\bar{p}\tau}}{k_{\bar{p}\tau}^2\theta_{\rm acc}}\right)^2. \quad (23)$$

Here $\theta_{\rm acc} \ll 1$ is the beam acceptance angle. According to definition of $\theta_{\rm acc}$, for scattering at smaller angles $\theta \leqslant \theta_{\rm acc}$ the antiprotons remain in the beam. The polarized total Coulomb cross sections σ_1^C and σ_2^C are zero for $\bar{p}\,^3$He scattering, since the nonrelativistic Coulomb elastic-scattering amplitude does not depend on the spins of $\bar{p}$ and ^{3}He and, in contrast to pp scattering, does not contain antisymmetrization terms. The remaining part of the Coulomb effects is related to Coulomb-nuclear interference. The spin structure of the $\bar{p}\,^3$He scattering amplitude is similar to that for pp scattering. Therefore, the cross sections due to the interference terms, $\sigma_0^{\rm int}$, $\sigma_1^{\rm int}$, and $\sigma_2^{\rm int}$, are calculated here on the basis of the formalism developed in Refs. [4,19]. The final result for $\bar{p}\,^3$He can be obtained from the one for $\bar{p}p$ scattering given in Eq. (27) of Ref. [19] via the following substitutions: $\alpha \to 2\alpha$, $m_p/2 \to \mu_{\bar{p}\tau}$, $\chi_0 \to \tilde{\sigma}_0$. Furthermore, the zero-angle helicity amplitudes $M_i^p(0)$ $(i = 1,2,3)$ of the hadronic $\bar{p}p$ scattering have to be replaced by the corresponding helicity amplitudes of zero-angle $\bar{p}\,^3$He scattering. When using the single-scattering approximation given by Eqs. (16), one finds the following expressions for the contribution of the Coulomb-nuclear interference terms to the total cross sections:

$$\begin{aligned}
\sigma_0^{\rm int} &= -\frac{2\pi}{k_{\bar{p}N}}\{\cos 2\tilde{\sigma}_0[-\sin\Psi\,{\rm Re}\tilde{M}_0 + (1-\cos\Psi){\rm Im}\tilde{M}_0] \\
&\quad - \sin 2\tilde{\sigma}_0[\sin\Psi\,{\rm Im}\tilde{M}_0 + (1-\cos\Psi){\rm Re}\tilde{M}_0]\}, \\
\sigma_1^{\rm int} &= -\frac{2\pi}{k_{\bar{p}N}}\big\{\cos 2\tilde{\sigma}_0\big[\sin\Psi\,{\rm Re}M_2^n(0) - (1-\cos\Psi){\rm Im}M_2^n(0)\big] \\
&\quad + \sin 2\tilde{\sigma}_0\big[\sin\Psi\,{\rm Im}M_2^n(0) + (1-\cos\Psi){\rm Re}M_2^n(0)\big]\big\}, \\
\sigma_2^{\rm int} &= -\frac{2\pi}{k_{\bar{p}N}}\{\cos 2\tilde{\sigma}_0[-\sin\Psi\,{\rm Re}\tilde{M}_2 + (1-\cos\Psi){\rm Im}\tilde{M}_2] \\
&\quad + \sin 2\tilde{\sigma}_0[\sin\Psi\,{\rm Im}\tilde{M}_2 - (1-\cos\Psi){\rm Re}\tilde{M}_2]\}, \quad (24)
\end{aligned}$$

where the following notations are used:

$$\begin{aligned}
\tilde{M}_0 &= 2M_1^p(0) + 2M_3^p(0) + M_1^n(0) + M_3^n(0), \\
\tilde{M}_2 &= M_2^n(0) + M_3^n(0) - M_1^n(0), \\
\Psi &= 2\eta\ln\sin\theta_{\rm acc}/2. \quad (25)
\end{aligned}$$

III. RESULTS FOR $\bar{p}\,^3$He AND $\bar{p}\,^4$He BASED ON THE GLAUBER-SITENKO APPROACH

In the present investigation we use two $\bar{N}N$ models developed by the Jülich group. Specifically, we use the models A(BOX) introduced in Ref. [11] and D described in Ref. [13]. Starting point for both models is the full Bonn NN potential [45]; it includes not only traditional one-boson-exchange diagrams but also explicit 2π- and $\pi\rho$-exchange processes as well as virtual Δ excitations. The G-parity transform of this meson-exchange NN model provides the elastic part of the considered $\bar{N}N$ interaction models. In the case of model A(BOX) [11] (in the following referred to as model A) a phenomenological spin-, isospin-, and energy-independent complex potential of Gaussian form is added to account for the $\bar{N}N$ annihilation. It contains only three free parameters (the range and the strength of the real and imaginary parts of the annihilation potential), fixed in a fit to the available total and

integrated NN cross sections. In case of model D [13], the most complete $\bar{N}N$ model of the Jülich group, the $\bar{N}N$ annihilation into two-meson decay channels is described microscopically, including all possible combinations of π, ρ, ω, a_0, f_0, a_1, f_1, a_2, f_2, K, K^*—see Ref. [13] for details—and only the decay into multimeson channels is simulated by a phenomenological optical potential. Results for the total and integrated elastic ($\bar{p}p$) and charge-exchange ($\bar{p}p \to \bar{n}n$) cross sections and also for angular-dependent observables for both models can be found in Refs. [11,13,26]. Evidently, with model A as well as with D a very good overall reproduction of the low- and intermediate-energy $\bar{N}N$ data was achieved.

The unpolarized cross sections for $\bar{p}\,^3$He and $\bar{p}\,^4$He are calculated using the multiple-scattering theory of Glauber-Sitenko [24,30]. It is known that for proton scattering on nuclei this theory is only valid at fairly high energies, say, for energies from ∼1 GeV upward. This differs in case of the antiproton-nucleus interaction. Strong annihilation effects in the elementary $\bar{p}N$ interaction lead to a peaking of the $\bar{p}N$ elastic-scattering amplitude in forward direction already at very low energies and, therefore, render it suitable for application of the eikonal approximation, which is the basis of the Glauber-Sitenko theory. As a consequence, for antiproton reactions this theory can be applied at much lower energies, namely ∼50 MeV or even less [46]. For example, for $\bar{p}d$ scattering we found that the Glauber-Sitenko theory even seems to work at $T_{\rm lab} \sim 25$ MeV [19]. However, since the radii of ^{3}He and ^{4}He are smaller than that of the deuteron, it is possible that for $\bar{p}\,^3$He, and especially for $\bar{p}\,^4$He, scattering the onset of applicability of the Glauber-Sitenko theory could occur at somewhat higher energies. Thus, in order to explore the reliability of this theory it would be desirable to confront our results with experimental information. Unfortunately, for $\bar{p}\,^3$He, the only published experimental result in the considered energy region is a $\bar{p}\,^3$He reaction cross section at the beam energy of 19.6 MeV [28]. There is one more data point, namely the $\bar{p}\,^3$He annihilation cross section close to threshold [35], but this is certainly outside of the region where the Glauber-Sitenko theory can be used.

Indeed, the experimental situation for $\bar{p}\,^4$He is much better. In this case the PS179 collaboration has published results for integrated [31–35] as well as differential cross sections [36,37]. Thus, as a test we performed also calculations for this system within the Glauber-Sitenko approach. In those calculations we employ a Gaussian representation of the $\bar{p}N$-scattering amplitude in the form

$$f_{\bar{p}N}(q) = \frac{k_{\bar{p}N}\sigma_{\rm tot}^{\bar{p}N}(i+\alpha_{\bar{p}N})}{4\pi}\exp\left(-\beta_{\bar{p}N}^2 q^2/2\right), \quad (26)$$

where q is the transferred three-momentum. The parameters $\sigma_{\rm tot}^{\bar{p}N}$, $\alpha_{\bar{p}N}$, and $\beta_{\bar{p}N}^2$ are fixed from the spin-averaged amplitudes $f_{\bar{p}N}$ of the models A and D and given in Ref. [19]. We utilize the formalism of Ref. [30], where a Gaussian nuclear density is used and corrections from the center-of-mass motion are included. Furthermore, we take into account explicitly that the $\bar{p}p$- and $\bar{p}n$-scattering amplitudes differ. We adopt the nuclear radius $r = 1.37$ fm for ^{4}He [30] and 1.5 fm for ^{3}He [47]. The differential cross section we obtained for $\bar{p}\,^4$He scattering at 179.6 MeV is in rather good agreement with the data of Ref. [36] (see Fig. 1). We want to emphasize that no free parameters are involved in our calculation. For comparison, we examined also the formalism of Ref. [47], where the $\bar{p}N$-scattering amplitudes are evaluated exactly for the single-scattering mechanism but taken out of the loop integrals for pN ($\bar{p}$N) rescattering of higher order. This approximation works rather well for proton-^{3}He scattering at a few hundred MeV [47], but in the case of $\bar{p}\,^4$He scattering at 179.6 MeV its applicability seems to be limited to much smaller scattering angles ($\theta_{\rm c.m.} < 30^\circ$) as compared to the approach of Ref. [30], as is demonstrated in Fig. 1 (cf. the dash-dotted curve).

Results at 19.6 MeV are also shown in Fig. 1 and compared with experimental information from Ref. [37]. Obviously, even at this fairly low energy, corresponding to a beam momentum of $p_{\rm lab} = 192.8$ MeV/c, the data are remarkably well reproduced. There is, however, an overestimation of the differential cross section at very forward angles. We included the Coulomb amplitude given by Eq. (22) in addition to the hadronic Glauber-Sitenko $\bar{p}^3$He amplitude and found that

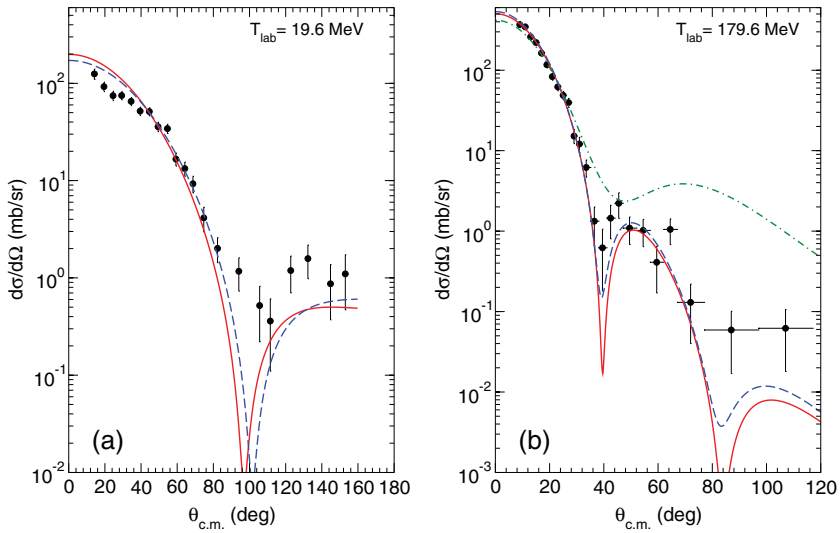

FIG. 1. (Color online) Differential cross section for $\bar{p}\,^4$He versus the center-of-mass scattering angle at $T_{\rm lab} = 19.6$ and 179.6 MeV. The solid and dashed lines are results for the $\bar{N}N$ models D and A, respectively, obtained on the basis of the approach [30]. The dash-dotted line is the result obtained within the approximation [47] for the Jülich model D. Data are taken from Refs. [37] (19.6 MeV) and [36] (179.6 MeV).

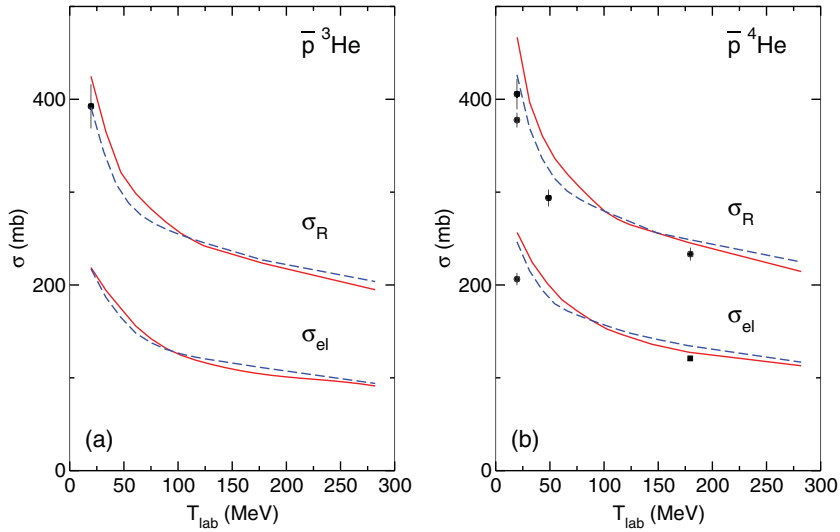

FIG. 2. (Color online) Integrated elastic ($\sigma_{\rm el}$, lower curves) and total reaction (σ_R, upper curves) cross sections for $\bar{p}\,^3$He and $\bar{p}\,^4$He versus the beam kinetic energy $T_{\rm lab}$. The solid and dashed lines are results for the $\bar{N}N$ models D and A, respectively, obtained on the basis of the Glauber-Sitenko approach [30]. Data for $\bar{p}\,^4$He are taken from Refs. [32] (filled circles), [36] (squares), and [37] (open circles). The data point for $\bar{p}\,^3$He is taken from Ref. [28].

at 19.6 MeV and scattering angles $\theta_{\rm c.m.}$ less than $\approx 2^\circ$ the Coulomb contribution is important but negligible at larger angles $\theta_{\rm c.m.} > 5^\circ$ and, therefore, does not allow one to explain the observed deviation in forward direction at 20°–40°.

The total cross section can be evaluated by using the optical theorem. At $T_{\rm lab} = 19.6$ MeV where the $\bar{p}\,^3$He reaction cross section was measured by the PS179 collaboration [28] we obtain $\sigma_0 = 609$ mb for model A and 644 mb for model D. Evaluating the differential cross section for elastic $\bar{p}\,^3$He scattering allows us to compute also the integrated elastic cross section $\sigma_{\rm el}$. Here we find $\sigma_{\rm el} = 217$ mb (A) and 219 mb (D). The reaction cross section is then given by $\sigma_R = \sigma_0 - \sigma_{\rm el}$ (we adopt here the notation of Ref. [33]). Thus, we get 392 mb for model A and 425 mb for model D. The experimental result is 392±23.8 mb [28]. It is quite remarkable that the Glauber-Sitenko theory combined with the Jülich models for the $\bar{p}N$ interaction agrees so well with the measurement at this low energy.

For $\bar{p}\,^4$He scattering experimental results for the reaction cross section [33] as well as for the integrated elastic cross section [36,37] have been published. Those data points are displayed in Fig. 2, together with the predictions of our calculations. One can see from the figure that the model results are well in line with the energy dependence exhibited by the data. But, in general, they overestimate the measured cross sections by 5 to 10% (model A) and 10 to 20% (model D). In the case of $\bar{p}\,^3$He, also shown in Fig. 2, the predictions for both considered $\bar{N}N$ models agree with the experiment within the error bars, as was already pointed out above. For completeness, predictions for the differential cross section for $\bar{p}\,^3$He scattering at two energies are displayed in Fig. 3. The results are qualitatively rather similar to those for the $\bar{p}\,^4$He system.

Finally, let us discuss here the so-called shadowing effects, i.e., the corrections that arise in the multiple-scattering approach of Glauber-Sitenko as employed in our calculation of the $\bar{p}\,^3$He and $\bar{p}\,^4$He scattering observables presented above. To determine the magnitude of the $\bar{p}N$ multiple-scattering contributions quantitatively, let us consider the ratio of the total $\bar{p}\,^3$He cross section obtained within the single-scattering approximation to the one accounting for all allowed orders of rescattering, $R = \sigma_0^{IA}/\sigma_0$. We found that this ratio is roughly

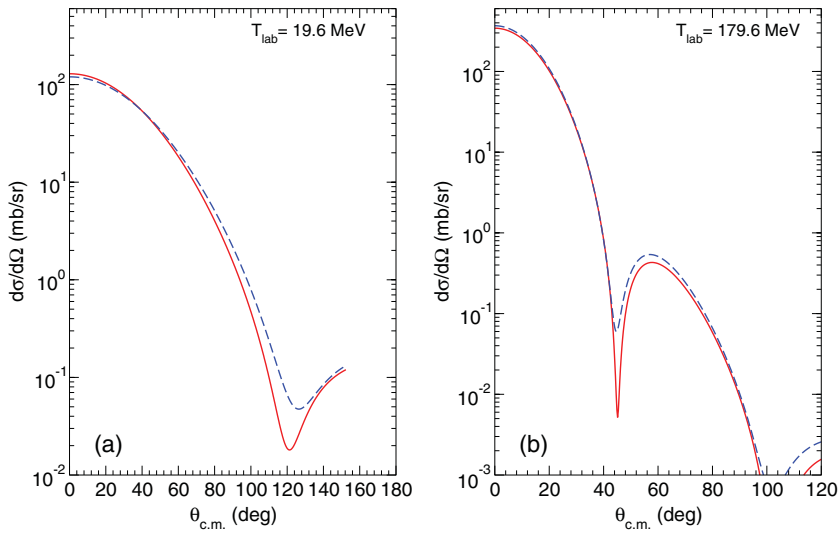

FIG. 3. (Color online) Differential cross section for $\bar{p}\,^3$He versus the center-of-mass scattering angle at $T_{\rm lab} = 19.6$ and 179.6 MeV. The solid and dashed lines are results for the $\bar{N}N$ models D and A, respectively, obtained on the basis of the approach [30].

1.45 at low energies ∼25 MeV and smoothly decreases to $R = 1.33$ when the beam energy is increased to 179.6 MeV. For $\bar{p}d$ scattering this ratio was found to be smaller, namely ∼1.1–1.15 [19]. The reason for this difference is the more compact structure of the ^{3}He as compared to the loosely bound deuteron, which leads to an increase of the shadowing effects. Indeed, this can be easily verified by simply increasing the radius of the Gaussian density r to 4 fm in our calculation. The ratio R then smoothly reduces to 1.15 at 19.6 and 1.09 at 179.6 MeV.

IV. POLARIZED CROSS SECTIONS FOR $\bar{p}\,^3$He

According to the analysis of the kinetics of polarization [4,6], the polarization buildup is determined mainly by the ratio of the polarized total cross sections (σ_1, σ_2) to the unpolarized one (σ_0) [4]. Let us define the unit vector $\boldsymbol{\zeta} = \mathbf{P}_T/P_T$, where $\mathbf{P}_T = \mathbf{P}_\tau$ is the target polarization vector, which enters Eq. (4). The nonzero antiproton beam polarization vector $\mathbf{P}_{\bar{p}}$, produced by the polarization buildup, is collinear to the vector $\boldsymbol{\zeta}$ for any directions of $\mathbf{P}_T$ and can be calculated from consideration of the kinetics of polarization. The general solution for the kinetic equation for $\bar{p}p$ scattering is given in Ref. [4]. Here we assume that this solution is valid for $\bar{p}\,^3$He scattering as well. Therefore, for the spin-filtering mechanism of the polarization buildup the polarization degree at the time t is given by [4,20]

$$P_{\bar{p}}(t) = \tanh\left[\frac{t}{2}(\Omega_-^{\rm out} - \Omega_+^{\rm out})\right], \tag{27}$$

where

$$\Omega_\pm^{\rm out} = nf\{\sigma_0 \pm P_T[\sigma_1 + (\boldsymbol{\zeta}\cdot\hat{\mathbf{k}})^2\sigma_2]\}. \tag{28}$$

Here n is the areal density of the target and f is the beam revolving frequency. Assuming the condition $|\Omega_-^{\rm out} - \Omega_+^{\rm out}| \ll (\Omega_-^{\rm out} + \Omega_+^{\rm out})$, which was found in Refs. [4,20] for $\bar{p}p$ scattering in storage rings at $n = 10^{14}$ cm^{-2} and $f = 10^6$ c^{-1}, one can simplify Eq. (27). If one denotes the number of antiprotons in the beam at the time moment t as $N(t)$, then the figure of merit is $P_{\bar{p}}^2(t)N(t)$. This value is maximal at the time $t_0 = 2\tau$, where τ is the beam lifetime, which is determined by the total cross section σ_0 of the interaction of the antiprotons with the nuclear target,

$$\tau = \frac{1}{nf\sigma_0}. \tag{29}$$

To estimate the efficiency of the polarization buildup mechanism it is instructive to calculate the polarization degree $P_{\bar{p}}$ at the time t_0 [20]. With our definition of σ_1 and σ_2 this quanitity is given by

$$P_{\bar{p}}(t_0) = -2P_T\frac{\sigma_1}{\sigma_0}, \quad \text{if } \boldsymbol{\zeta}\cdot\hat{\mathbf{k}} = 0,$$
$$P_{\bar{p}}(t_0) = -2P_T\frac{\sigma_1+\sigma_2}{\sigma_0}, \quad \text{if } |\boldsymbol{\zeta}\cdot\hat{\mathbf{k}}| = 1. \tag{30}$$

Let us first look at the spin-dependent cross sections themselves which are presented in Fig. 4. Note that here the corresponding calculations are all done in the single-scattering approximation only, as described in Secs. II B and IIIC. The center-of-mass acceptance angle used in those calculations is $\theta_{\rm acc} = 10$ mrad. In principle, the corrections from multiple scattering to the spin-dependent cross sections could be worked out by extending the formalism described in Refs. [48] to the $\bar{p}\,^3$He case. We expect that the multiple-scattering effects on those quantities are roughly of the same magnitude (i.e., around 30% for energies above 20 MeV) as for the spin-independent cross sections. This was found in the case of $\bar{p}d$, at least, reported in Ref. [22]. Therefore, we believe that the single-scattering approximation provides a reasonable estimation for the magnitude of the polarization-build-up effect in $\bar{p}\,^3$He scattering and we refrain from a thorough evaluation of the involved multiple-scattering effects in the present analysis. After all, one has to keep in mind that the differences between the $\bar{N}N$ models A and D introduce

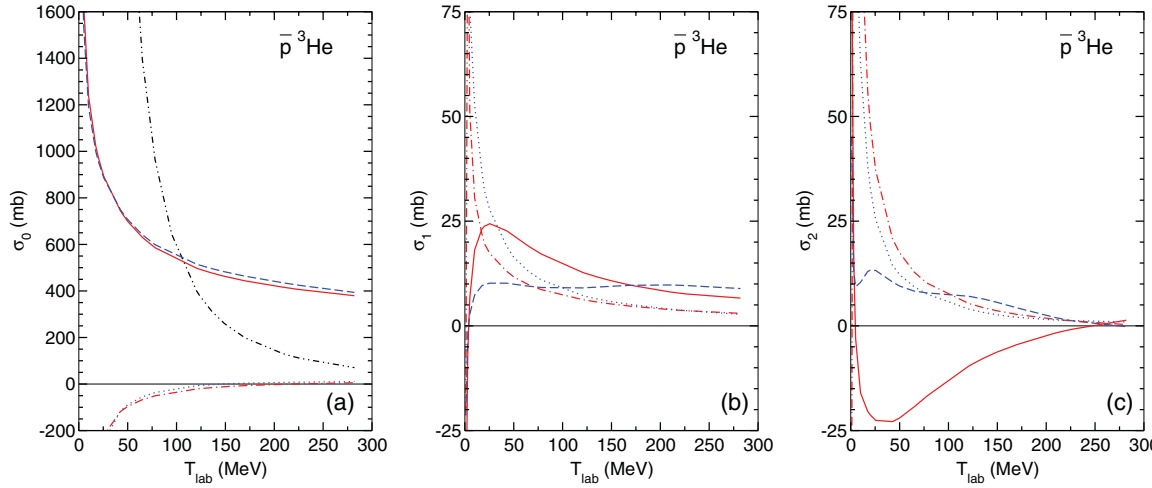

FIG. 4. (Color online) Total cross sections σ_0, σ_1, and σ_2 versus the antiproton laboratory energy $T_{\rm lab}$ for $\bar{p}\,^3$He scattering. Results based on the purely hadronic amplitude, σ_i^h [(solid line) model D; (dashed line) model A] and for the Coulomb-nuclear interference term, $\sigma_i^{\rm int}$ [(dash-dotted line) model A; (dotted line) model D], are presented. In case of σ_0 the Coulomb cross section [cf. Eq. (23)] is shown too (dash-double-dotted line). The employed acceptance angle is $\theta_{\rm acc} = 10$ mrad.

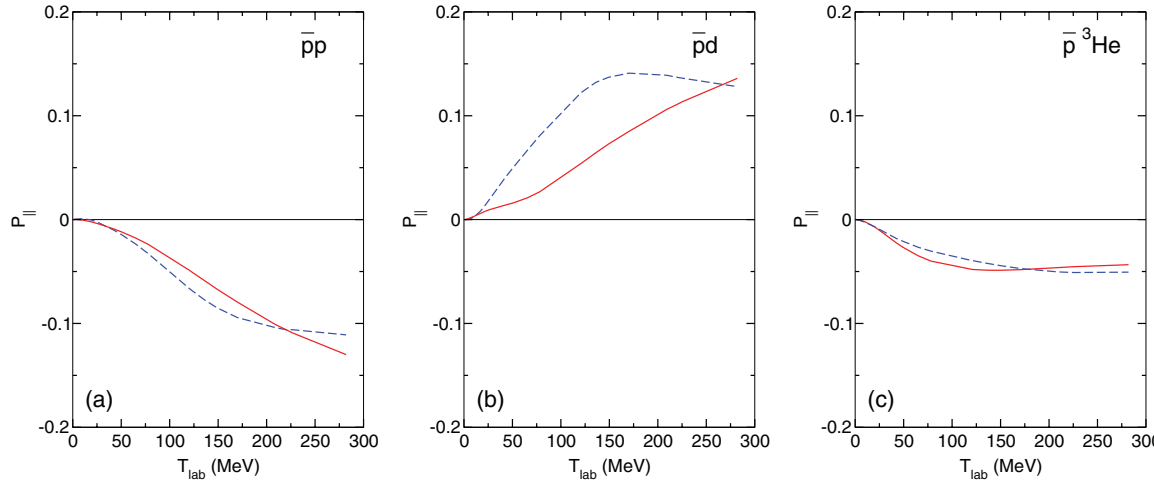

FIG. 5. (Color online) Dependence of the longitudinal polarization $P_{||}$ (i.e., $P_{\bar{p}}(t_0)$ for $\boldsymbol{\zeta}\cdot\hat{\mathbf{k}}=1$) on the beam energy for the target polarization $P_T=1$ in the different reactions $\bar{p}p$, $\bar{p}d$, and $\bar{p}\,^3$He. The results are for models A (dashed line) and D (solid line). The employed acceptance angle is $\theta_{\rm acc}=10$ mrad.

significantly larger variations in the cross sections σ_1 and σ_2, cf. Fig. 4.

Our results suggest that the magnitude of the spin-dependent cross sections σ_1 and σ_2 for $\bar{p}\,^3$He are comparable to those for $\bar{p}p$ and $\bar{p}d$, at least as far as the hadronic part is concerned. However, due to the larger charge of ^{3}He, Coulomb-nuclear interference effects turn out to be more important. Indeed, the Coulomb-nuclear interference cross sections $\sigma_i^{\rm int}$ are comparable to the corresponding polarized hadronic cross sections σ_1 and σ_2 even at 100–200 MeV.

The unpolarized cross section σ_0^h (cf. left panel of Fig. 4) is roughly a factor 3 larger than the one for $\bar{p}p$ [19], as expected. Moreover, the Coulomb cross section is significantly larger than in the $\bar{p}p$ case. Indeed, the latter is still of similar magnitude as the purely hadronic cross section σ_0^h at beam energies around 100 MeV.

The polarization degree $P_{\bar{p}}(t_0)$ for $\boldsymbol{\zeta}\cdot\hat{\mathbf{k}}=1$ ($P_{||}$) at $P_T=P^d=1$ for $\bar{p}\,^3$He is shown in Fig. 5 versus the beam energy. The results for $\boldsymbol{\zeta}\cdot\hat{\mathbf{k}}=0$ ($P_\perp$) are displayed in Fig. 6. For the ease of comparison the polarization degree for the $\bar{p}p$ and $\bar{p}d$ cases [21] are included as well. The magnitudes of $P_{||}$ and $P_\perp$ in the region of the beam energy 0–300 MeV are in the order of 5% . In the case of $P_{||}$ they tend to be smaller than those predicted for $\bar{p}p$ [20,21] and $\bar{p}d$ [21,22], whereas for $P_\perp$ they are comparable to the ones for those other antiproton reactions.

Since the polarization degree for $\bar{p}n$ was found to be on the order of 20% [21] one might naively expect that it could be similar for ^{3}He because, as mentioned above, in the latter the polarization is carried mainly by the neutron. However, the polarization degree is determined by the ratios of the spin-dependent cross sections $\sigma_i=\sigma_i^h+\sigma_i^{\rm int}$ ($i=1,2$) to $\sigma_0=\sigma_0^h+\sigma_0^{\rm int}+\sigma_0^C$, cf. Eq. (30) and, thus, is reduced by the larger

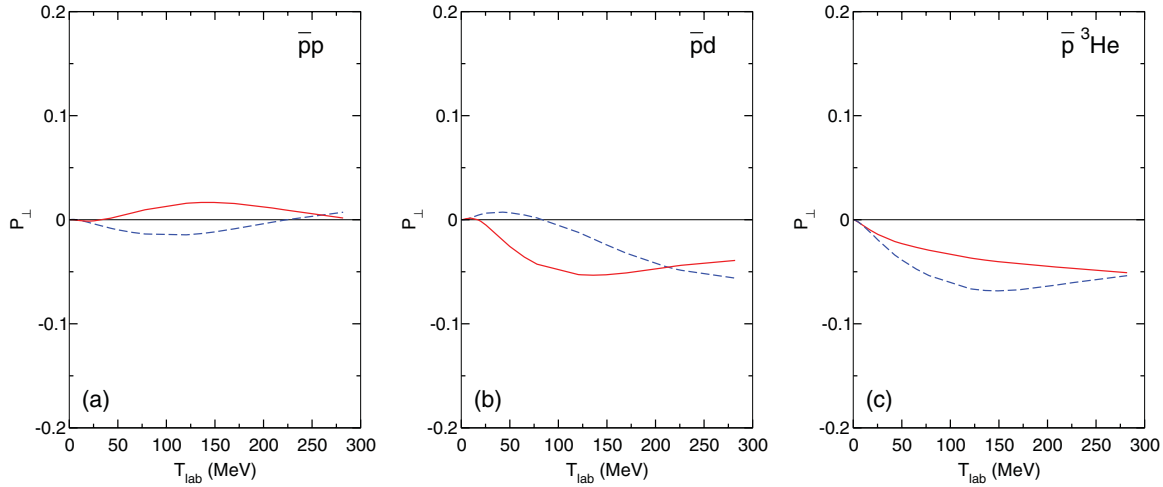

FIG. 6. (Color online) Dependence of the transversal polarization $P_\perp$ [i.e., $P_{\bar{p}}(t_0)$ for $\boldsymbol{\zeta}\cdot\hat{\mathbf{k}}=0$] on the beam energy for the target polarization $P_T=1$ in the different reactions $\bar{p}p$, $\bar{p}d$, and $\bar{p}\,^3$He. The results are for models A (dashed line) and D (solid line). The employed acceptance angle is $\theta_{\rm acc}=10$ mrad.

unpolarized cross section σ_0 and, in particular, the larger total Coulomb cross section σ_0^C in the $\bar{p}\,^3$He system. In this context, note that also the beam lifetime decreases with increasing σ_0; see Eq. (29).

As discussed in Sec. III, if one goes beyond the single-scattering approximation the hadronic part of the unpolarized cross section σ_0^h decreases by a factor of $\approx$1.4 which, in principle, would lead to an increase of the polarization efficiency by the same factor. However, in the case of $\bar{p}d$ it also has been found that the spin-dependent cross sections are reduced [22] by a similar amount so there is practically no net effect. It is likely that the same will happen for $\bar{p}\,^3$He as well.

V. SUMMARY

In the present article we employed two $\bar{N}N$ potential models developed by the Jülich group for a calculation of $\bar{p}\,^3$He and $\bar{p}\,^4$He scattering within the Glauber-Sitenko theory. One of the aims was to examine in how far antiproton scattering off a polarized ^{3}He target would be suitable for obtaining a polarized antiproton beam via the spin-filtering method. The predicted spin-dependent cross sections for $\bar{p}\,^3$He, evaluated in the single-scattering approximation for the Jülich $\bar{N}N$ models A and D, are comparable to those for the scattering of antiprotons on polarized ^{1}H or deuteron targets. However, since the total cross section is larger in the case of ^{3}He, the resulting efficiency of the polarization buildup tends to be somewhat smaller than those for $\bar{p}p$ and $\bar{p}d$ so one has to conclude that the use of a polarized ^{3}He target might be less favorable for obtaining a polarized beam of antiprotons as required for the PAX experiment.

In addition to the issue of the polarization buildup for antiprotons, $\bar{p}\,^3$He scattering is interesting for studying the spin dependence of the elementary $\bar{p}N$ amplitudes. Since the spin-dependent part of $\bar{p}\,^3$He scattering is determined mainly by the $\bar{p}n$ amplitude, scattering of antiprotons on a polarized $\bar{p}\,^3$He target could reveal valuable additional information on this amplitude. It would supplement the constraints that could be provided by the expected data on $\bar{p}d$ scattering from the AD experiment [27], since in the latter a stronger interplay between the $\bar{p}p$ and $\bar{p}n$ amplitudes has to be expected. Our results for unpolarized observables (integrated and differential cross sections) for $\bar{p}\,^3$He and $\bar{p}\,^4$He, obtained within the Glauber-Sitenko approach, agree rather well with the available experimental information in the energy range from 20 MeV upward. We view this as a strong indication that this formalism is suited for analyzing data for those reactions in the low- and intermediate-energy regions. Of course, once concrete measurements with polarizated beam or target are planned, our calculations have to be improved and, specifically, corrections due to multiple scattering have to be also taken into account in the computation of polarization observables.

ACKNOWLEDGMENTS

We acknowledge stimulating discussions with N. N. Nikolaev and F. Rathmann. Furthermore, we thank A. Kudryavtsev for help with getting access to some of the literature. This work was supported in part by the Heisenberg-Landau program.

[1] V. Barone *et al.* (PAX Collaboration), arXiv:hep-ex/0505054.
[2] F. Rathmann *et al.*, Phys. Rev. Lett. **94**, 014801 (2005).
[3] F. Rathmann *et al.*, Phys. Rev. Lett. **71**, 1379 (1993).
[4] A. I. Milstein and V. M. Strakhovenko, Phys. Rev. E **72**, 066503 (2005).
[5] N. N. Nikolaev and F. Pavlov, arXiv:hep-ph/0512051.
[6] N. N. Nikolaev and F. Pavlov, AIP Conf. Proc. **915**, 932 (2007).
[7] N. N. Nikolaev and F. Pavlov, AIP Conf. Proc. **1008**, 34 (2008).
[8] C. B. Dover and J. M. Richard, Phys. Rev. C **21**, 1466 (1980); **25**, 1952 (1982).
[9] J. Côté, M. Lacombe, B. Loiseau, B. Moussallam, and R. Vinh Mau, Phys. Rev. Lett. **48**, 1319 (1982).
[10] P. H. Timmers, W. A. van der Sanden, and J. J. de Swart, Phys. Rev. D **29**, 1928 (1984).
[11] T. Hippchen, J. Haidenbauer, K. Holinde, and V. Mull, Phys. Rev. C **44**, 1323 (1991).
[12] R. Timmermans, Th. A. Rijken, and J. J. de Swart, Phys. Rev. C **50**, 48 (1994).
[13] V. Mull and K. Holinde, Phys. Rev. C **51**, 2360 (1995).
[14] B. El-Bennich, M. Lacombe, B. Loiseau, and S. Wycech, Phys. Rev. C **79**, 054001 (2009).
[15] C. Amsler and F. Myhrer, Annu. Rev. Nucl. Part. Sci. **41**, 219 (1991).
[16] C. B. Dover, T. Gutsche, M. Maruyama, and A. Faessler, Prog. Part. Nucl. Phys. **29**, 87 (1992).
[17] E. Klempt, F. Bradamante, A. Martin, and J.-M. Richard, Phys. Rep. **368**, 119 (2002).
[18] V. F. Dmitriev, A. I. Milstein, and V. M. Strakhovenko, Nucl. Instrum. Methods B **266**, 1122 (2008).
[19] Yu. N. Uzikov and J. Haidenbauer, Phys. Rev. C **79**, 024617 (2009).
[20] V. F. Dmitriev, A. I. Milstein, and S. G. Salnikov, Phys. Lett. B **690**, 427 (2010).
[21] Yu. N. Uzikov and J. Haidenbauer, J. Phys. Conf. Ser. **295**, 012087 (2011).
[22] S. G. Salnikov, arXiv:1106.4887 [hep-ph].
[23] R. J. Glauber and G. Matthiae, Nucl. Phys. B **21**, 135 (1970).
[24] A. G. Sitenko, Fiz. Elem. Chastits At. Yadra **4**, 546 (1973) [Sov. J. Part. Nuclei **4**, 231 (1973)].
[25] V. Mull, J. Haidenbauer, T. Hippchen, and K. Holinde, Phys. Rev. C **44**, 1337 (1991).
[26] J. Haidenbauer, J. Phys. Conf. Ser. **295**, 012094 (2011).
[27] C. Barschel *et al.* (PAX Collaboration), arXiv:0904.2325 [nucl-ex].
[28] F. Balestra *et al.*, Phys. Lett. B **215**, 247 (1988).
[29] A. Bianconi *et al.*, Phys. Lett. B **492**, 254 (2000).
[30] W. Czyż and L. Leśniak, Phys. Lett. B **24**, 227 (1967).
[31] F. Balestra *et al.*, Phys. Lett. B **149**, 69 (1984).
[32] F. Balestra *et al.*, Phys. Lett. B **165**, 265 (1985).
[33] F. Balestra *et al.*, Phys. Lett. B **194**, 343 (1987).
[34] F. Balestra *et al.*, Nuovo Cimento A **100**, 323 (1988).

[35] F. Balestra *et al.*, Phys. Lett. B **230**, 36 (1989).
[36] Yu. A. Batusov *et al.*, Sov. J. Nucl. Phys. **52**, 776 (1990).
[37] F. Balestra *et al.*, Phys. Lett. B **305**, 18 (1993).
[38] A. Zenoni *et al.*, Phys. Lett. B **461**, 413 (1999).
[39] L. A. Kondratyuk and M. Zh. Shmatikov, Yad. Fiz. **38**, 361 (1983) [Sov. J. Nucl. Phys. **38**, 216 (1983)].
[40] G. Bendiscioli, A. Rotondi, and A. Zenoni, Nuovo Cimento A **105**, 1055 (1992).
[41] P. La France and P. Winternitz, J. Phys. (France) **41**, 1391 (1980).
[42] J. Bystricky, F. Lehar, and P. Winternitz, J. Phys. (France) **39**, 1 (1978).
[43] A. G. Sitenko and V. F. Kharchenko, Usp. Fiz. Nauk **103**, 469 (1971).
[44] L. D. Landau and E. M. Lifshits, *Quantum Mechanics: Non-Relativistic Theory* (Pergamon, Oxford, 1965).
[45] R. Machleidt, K. Holinde and Ch. Elster, Phys. Rep. **149**, 1 (1987).
[46] L. A. Kondratyuk, M. Zh. Shmatikov, and R. Bizzarri, Yad. Fiz. **33**, 795 (1981) [Sov. J. Nucl. Phys. **33**, 413 (1981)].
[47] D. K. Hasell *et al.*, Phys. Rev. C **34**, 236 (1986).
[48] M. N. Platonova and V. I. Kukulin, Phys. Rev. C **81**, 014004 (2010).